generating output power in excess of 120watt with over all wall plug efficiency of about 1.4 %. Both the CVL units were optically aligned, electronically synchronized and optimized to achieve about 125watt total output power from this oscillatoramplifier configuration. The beam of KE-CVL oscillator with output power of about 20watt was folded and fed into the KE-CVL amplifier to achieve 125watt output power from the system. The tuning curve of amplifier (fig. L.8.2) was 150ns broad with FWHM of about 100ns . This is about 30 % more in comparison to that of standard CVLs. The amplifier contribution was about 105watt and hence the electro-optical efficiency of the KE-CVL amplifier was about ~ 1.6 %. The total input power to the oscillator and amplifier (both) units was about 9kW with total laser output power of ~ 125watt (maximum). The over all wall plug efficiency of the configuration was about 1.4 %.

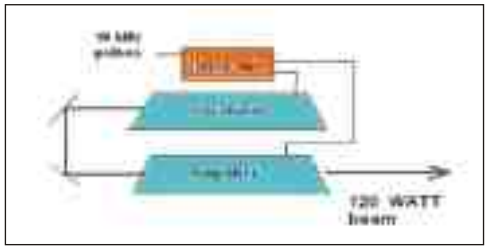

Fig. L.8.1 *Schematic of oscillator amplifier configuration.*

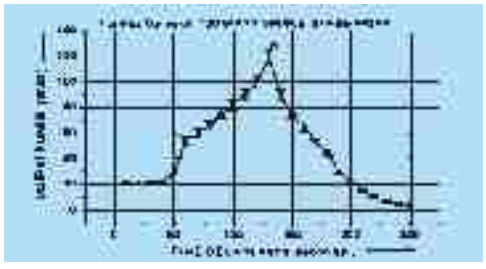

Fig. L.8.2 *Tuning of the oscillator amplifier.*

Fig. L.8.3 *Experimental layout of the KE-CVLs in oscillator-amplifier configuration.*

Contributed by:
B. Singh; bsingh @cat.ernet.in

L.9 Cation size effect on the Hyper-Rayleigh scattering and continuum generation of salt induced aggregates of silver nanoparticles

Research has been initiated on the use of nanomaterials for various bio-medical applications at Laser Biomedical Applications & Instrumentation Division. We have started preparing and characterizing metallic nanoparticles (NPs) of silver and gold because of their interesting size-dependent optical and electronic properties. One such nonlinear optical property of these metallic NPs is hyper-Rayleigh scattering (HRS). This is due to incoherent second harmonic generation (SHG) from the nanoparticle-solution interface.

HRS can be used as a sensitive tool to probe the salt induced aggregation of the metallic NPs as their aggregates show an order of magnitude increase in the HRS intensities. Addition of salts reduces the thickness of the electrical double layer (EDL) surrounding a NP, thereby reducing the electrostatic repulsion, which results in increased rate of aggregation. According to Gouy-Chapman model, for a 1:1 electrolyte the thickness of the EDL around a colloidal particle is dependent only on the ionic concentration and not on the ionic size. However, we have found that the effect of cation size (Li^+, Na^+ and K^+; chloride counterion) plays a profound role on the aggregation behavior of silver NPs (AgNPs). The AgNPs prepared had a SPR (surface plasmon resonance) band centered at 400nm having a size distribution of 20±5nm. The effect of addition of salts on the HRS intensities is observed to depend markedly upon the size of the cation (fig. L.9.1). For larger cations, Na^+ and K^+ the HRS intensities increase considerably (50 times) as the electrolyte concentration is increased beyond ~50mM. However for Li^+ this increase is only nominal (~ 4 times). Continuum generation was also observed upon addition of NaCl or KCl, but not in presence of LiCl. Fig. L.9. 2 shows the continuum spectra along with the transmission curve of the bandpass filter used to record the continuum and HRS signals. It is evident that the transmission properties of the filter used restrict the measured spectral extent of the observed continuum towards red. Although all the three cations have same charge, Li^+ has the smallest size, which means it has the highest charge density. These observations suggest that smaller size and hence higher ionic charge density of the Li^+ ion is not conducive to the formation of aggregates. Our observation can be related to the "Hofmeister effect", which describes the relative effectiveness of anions or cations, on a wide range of phenomena including colloidal aggregation. Further studies are in progress to understand the nonlinear optical properties of these salt induced aggregates.

[*For further details, see K. Das, A. Uppal, P. K. Gupta, Chemical Physics. Letters, Volume 426, page 155, 2006]*

Fig. L.9.1 Relative change in HRS signals intensity of the AgNPs upon addition of the salts. (Incident laser power at 800nm: 50mW).

Fig. L.9. 2 HRS and continuum spectra of Ag NPs upon addition of 50mM NaCl. (Laser power at 800nm: 50mW). Also shown are spectra for bare and LiCl added AgNPs and the transmission curve of the bandpass filter used.

Contributed by:
K. Das; kaustuv@cat.ernet.in

L.10 Development of a handheld probe for real time imaging using optical coherence tomography

Optical coherence tomography (OCT) has emerged as an attractive technique for real time depth resolved cross-sectional imaging of biological tissues with micrometer-scale resolutions. OCT relies on the principle of low coherence interferometry, wherein light from a broadband source backscattered from a sample is mixed with the reference light using Michelson interferometer geometry. Interference takes place only when the sample arm path length matches exactly the reference arm path within the coherence length of the source. This allows probing different layers of the sample. Two-dimensional cross sectional imaging is achieved by performing successive axial measurements at different transverse positions. Previously a single mode fiber optic based optical coherence tomography system has been developed at Laser Biomedical Applications & Instrumentation Division, which is being used for in-vitro and in-vivo imaging of biological tissues. This setup can take axial scans at the rate of ~1Hz leading to typical image acquisition time of a minute or so. In order to acquire OCT images at video rate, a high speed OCT setup was developed with 1310nm broadband light source. The diode output was coupled into a fiber optic based Michelson interferometer by use of a 3-dB bi-directional fused fiber coupler designed for the wavelength used. The reference arm consists of a Fourier domain rapid scanning optical delay line using a resonant scanning mirror oscillating at 2KHz. Lateral scanning was done using a galvo scanner. The sample arm was designed to be in the form of a hand-held probe. The light incident on the galvo scanner was relayed with a pair of lenses and focused on to the sample using an objective lens. The light reflected from both the sample and reference arms was detected by a photodiode and the resulting interferogram was filtered and demodulated using a logarithmic amplifier and digitized using a frame grabber board. Two-dimensional OCT images were formed by lining up successive axial (depth) -scans and 2-D images were displayed on PC. Data was acquired from both the forward and reverse scans with an effective axial scan rate of 4KHz. The setup was designed to acquire images at the rate of 8 frames/sec. The axial and lateral resolutions of the setup in free space were ~18μm. The hand-held probe as shown in the picture is easily accessible for imaging skin of the human body. This setup is expected to have potential clinical applications in dermatology.

Fig. L.10.1 Photograph of the hand held OCT probe for dermal imaging.

Contributed by:
K.Divakar Rao; kdivakar@cat.ernet.in

L.11 Trapping of micron sized objects near a free liquid surface

It is difficult to manipulate objects near a free liquid surface with conventional optical tweezers because of the limited working distance available with the high numerical aperture objectives used in optical tweezers. We have shown that the thermocapillary effect, which arises due to the changes in surface tension of free liquid surface by laser induced heating, can be exploited for such applications.

The approach exploits the fact that the trap laser beam focused at a free liquid surface, results in an axi-symmetric temperature distribution at the surface having a